Eur. Phys. J. B **11**, 559–564 (1999)

**THE EUROPEAN PHYSICAL JOURNAL B**

EDP Sciences


# Ab initio calculation of local vibrational modes by the Green's function method. Application to GaAs:C and GaN:As

C. Göbel, K. Petzke, C. Schrepel, and U. Scherz[a]

Institut für Theoretische Physik, Technische Universität Berlin, Hardenbergstrasse 36, 10623 Berlin, Germany

Received 5 March 1999

**Abstract.** We present an *ab initio* technique for the calculation of vibrational modes at deep defects in semiconductors outside and inside the host-phonon bands. The dynamical matrix is calculated using density-functional theory in the local density approximation. In the results presented here all interatomic harmonic forces up to the eleventh nearest neighbour of a particular atom of the perturbed or unperturbed crystal are included. The Green's function method is used to obtain the difference of the density of phonon states between the perturbed and the perfect crystal. This technique is applied to calculate the split-off mode at the C impurity at As site in GaAs and its isotope shifts, which are in good agreement with Raman scattering experiments. It is demonstrated that the impurities generate resonances and localized modes inside the host-phonon bands. The resonances arise at specific energies of the density of phonon states of the perfect crystal which are practically independent of the chemical nature of the defect, whereas the localized modes show distinct impurity or ligand isotope shifts. Our calculations of GaAs and cubic GaN lead to the assignment of a number of low energy Raman-scattering peaks between 7.2 meV and 31.0 meV, observed at a layer of cubic GaN on a GaAs substrate, to resonances inside the phonon bands of GaAs and GaN.

**PACS.** 63.20.Pw Localized modes – 78.30.Fs III-V and II-VI semiconductors

## 1 Introduction

The investigation of local vibrational modes, observed by Raman scattering or infrared spectroscopy, provides important information about defects in semiconductors. In order to understand the atomic structure of the defect, the location of the impurity or the atoms of a defect complex, as well as the relaxation of the nearest neighbours, it is necessary to perform *ab initio* calculations of the interatomic forces and to compare the resulting energies of the modes with the measured values.

The incorporation of an impurity into a semiconductor crystal may not only generate local vibrational modes (LVM) in the gap between host-phonon bands or split-off modes above the optical phonon bands, but also causes resonances and localized vibrations inside the bands. In case of GaAs:C, for example, the carbon impurity has a much lighter mass than the replaced arsenic and a LVM is observed, whose energy is well above the energy of the highest optical phonon band. In this case the hybridization with crystal phonons is small, resulting in pronounced energy shifts of the LVM for different impurity or ligand isotopes. In addition, a number of resonances are found in the difference of the density of phonon states (DDPS) between the perfect and the perturbed crystal, and also distinct localized modes. The resonances are seen at specific energetic positions of the density of phonon states (DPS) of the perfect crystal, whereas the localized modes are characteristic for the defect.

In case of cubic GaN:As, however, a LVM at the As impurity, replacing a much lighter nitrogen atom, can not occur as a split-off mode but is found in the band gap between the acoustical and optical phonon bands. There are also a number of resonances inside the acoustical and optical phonon bands and distinct localized modes below the upper edge of the acoustical phonon band.

The calculation of vibrational modes, caused by deep defects, is based on the correct determination of the phonons of the perfect crystal. Such *ab initio* calculations had been done by density-functional perturbation theory [1] and by the direct calculation of the dynamical matrix using density-functional theory [2,3], and excellent agreement has been achieved in both cases with phonon dispersion curves from neutron-scattering experiments for various semiconductors. In case of a crystal containing a defect, however, the situation is much more complicated. The change of the interatomic forces in the vicinity of the defect causes a relaxation of the nearby atoms and a long range lattice relaxation. As a result of the defect perturbation, the translational symmetry of the crystal is destroyed and localized vibrations arise, which may also depend on the impurity or ligand masses. In case of impurities with masses much smaller than the masses

[a] e-mail: scherz@physik.tu-berlin.de

of the replaced atoms very localized vibrations are formed with energies higher than the optical phonon band of the perfect crystal. In the other cases the number of atoms involved in localized vibrations may be very large. Nevertheless, from the experimental point of view, defect induced vibrations are observed from a comparison with the vibrational modes of the perfect crystal, which are usually also seen at the perturbed crystal.

The theoretical models therefore describe the defect induced vibrations as a perturbation of the perfect crystal and different localizations of the modes may be discussed in terms of different hybridizations of a local vibration with crystal phonons. Robbie *et al.* [4,5], for example, used *ab initio* results from density-functional linear-response theory to calculate the Green's function of the perfect crystal. The change of the force constants due to the perturbation with the defect was treated using a model with two parameters: nearest neighbour bond stretching $\alpha$ and bond bending $\beta$. From this model, a defect matrix was calculated, which accounted for the changes between the perfect and the disturbed system. The Dyson equation was used to calculate the Green's function of the disturbed system from the Green's function of the perfect crystal and the defect matrix. Because this model is not parameter-free, it cannot predict actual frequencies. In addition, Robbie *et al.* [4] showed that the magnitude of the change of the force constants, required to fit experimental results, strongly depends on the valence force model used. Therefore, such model calculations should be treated with caution.

Petzke *et al.* [6] used *ab initio* techniques for both the perfect and the disturbed system. They calculated the localized vibrations using a cluster of several hundred vibrating atoms around the defect. The cluster was embedded in a crystal at rest and the interatomic forces in the vicinity of the defect were obtained from *ab initio* calculations using density-functional theory. The vibration frequencies were found from the eigenvalues of the dynamical matrix and the LVMs were selected from their large vibration amplitudes of the atoms in the vicinity of the defect as obtained from the eigenvectors of the dynamical matrix. Alternatively, the LVMs can also be deduced from a comparison of the density of phonon states between two clusters, where one contains the defect and the other represents the perfect crystal. However, the cluster method has two disadvantages: Due to the final size of the cluster, the phonons with small wave vectors can not be described. Localized vibrations, which are calculated in the corresponding energy range, may be artificial. In addition to this problem, unphysical vibrations may appear at the surface of the cluster.

For best results, the Green's function technique should be used in conjunction with *ab initio* calculations for both the perfect and disturbed system. Only this combined method allows to predict the frequencies of local and localized vibrational modes.

We here present *ab initio* calculations of the interatomic forces using density-functional theory and the supercell method, which is a generalization of the method of Frank *et al.* [7]. This technique is, however, not only applied to the perfect crystal, but also to the crystal containing a defect. The LVMs are then determined by the Green's function technique, developed by Maradudin [8]. The perturbation matrix, entering the Dyson equation, is calculated from the change of the force constants and masses due to the defect. The LVMs can then be determined from the singularities of the Green's function of the perturbed crystal. The difference of the density of phonon states (DDPS) between the perturbed and the unperturbed crystal additionally give the localized modes and resonances inside the phonon bands.

The paper is organized as follows: The Green's function technique is shortly summarized in Section 2, and Section 3 contains some details about the numerical procedure. The method is then applied in Section 4 to a LVM above the energies of the phonon bands and in Sections 5 and 6 to localized modes at the edges of the phonon bands and to resonances inside the phonon bands.

## 2 Green's function method

Following the derivation of Maradudin [8] the cartesian component $\alpha$ of the displacement of the $i$th atom in the $n$th unit cell is denoted by $u_{ni\alpha}$ and $M_{ni}$ are the masses of the corresponding atoms. Then, in the classical approximation the equation of motion of the perturbed crystal is given by

$$M_{ni}\ddot{u}_{ni\alpha} + \sum_{n',i',\alpha'} \underset{\alpha\alpha'}{\Phi^{nn'}_{ii'}} u_{n'i'\alpha'} = 0, \tag{1}$$

where $\underset{\alpha\alpha'}{\Phi^{nn'}_{ii'}}$ are the force constants in the harmonic approximation. Introducing the masses $m_i$ and force constants $\underset{\alpha\alpha'}{\phi^{nn'}_{ii'}}$ of the perfect crystal, the change of masses due to the impurities is

$$\Delta m_{ni} = M_{ni} - m_i \tag{2}$$

and the change of the force constants is

$$\Delta\underset{\alpha\alpha'}{\phi^{nn'}_{ii'}} = \underset{\alpha\alpha'}{\Phi^{nn'}_{ii'}} - \underset{\alpha\alpha'}{\phi^{nn'}_{ii'}}. \tag{3}$$

The equation of motion of a crystal containing a defect may then be written in the form

$$m_i\ddot{u}_{ni\alpha} + \sum_{n',i',\alpha'} \underset{\alpha\alpha'}{\phi^{nn'}_{ii'}} u_{n'i'\alpha'} = \Delta m_{ni}\ddot{u}_{ni\alpha} + \sum_{n',i',\alpha'} \Delta\underset{\alpha\alpha'}{\phi^{nn'}_{ii'}} u_{n'i'\alpha'}. \tag{4}$$

The left hand side is the equation of motion of the perfect crystal and the right hand side is the perturbation due to different masses and different force constants of the defect. Because of the translational symmetry the dynamical matrix of the perfect crystal is written in the form

$$\underset{\alpha\alpha'}{D_{ii'}}(\mathbf{k}) = \sum_l \frac{1}{\sqrt{m_i m_{i'}}} \underset{\alpha\alpha'}{\phi^{0l}_{ii'}} \exp\left\{\mathrm{i}\mathbf{k}\cdot\mathbf{R}_l\right\}, \tag{5}$$

where $\mathbf{R}_l$ denotes the position of the $l$th unit cell and $\mathbf{k}$ is the wave vector. The square roots of the eigenvalues of the dynamical matrix are the vibration frequencies $\omega(j,\mathbf{k})$ of the normal mode $j$ and wave vector $\mathbf{k}$, and the corresponding eigenvectors $e_{i\alpha}(j,\mathbf{k})$ give the relative vibration amplitudes of the atoms.

The Green's function of the perfect crystal is given by

$$G_{0\substack{i\,i'\\ \alpha\alpha'}}^{nn'}(\omega^2) = \lim_{\varepsilon\to+0}\sum_{j,\mathbf{k}}\frac{X_{ni\alpha}(j,\mathbf{k})X^*_{n'i'\alpha'}(j,\mathbf{k})}{\omega^2-\omega^2(j,\mathbf{k})+i\varepsilon}, \quad (6)$$

with

$$X_{ni\alpha}(j,\mathbf{k}) = \frac{1}{\sqrt{N}}e_{i\alpha}(j,\mathbf{k})\exp\left\{\mathrm{i}\mathbf{k}\cdot\mathbf{R}_n\right\} \quad (7)$$

and $N$ denotes the number of unit cells. The density of phonon states of the perfect crystal is

$$g_0(\omega) = -\frac{1}{\pi}\sum_{n,i,\alpha}\mathrm{Im}\left\{G_{0\substack{i\,i\\ \alpha\alpha}}^{nn}(\omega^2)\right\}. \quad (8)$$

Introducing the perturbation matrix

$$C_{\substack{i\,i'\\ \alpha\alpha'}}^{nn'}(\omega^2) = \omega^2\frac{\Delta m_{ni}}{m_i}\delta_{nn'}\delta_{ii'}\delta_{\alpha\alpha'} - \frac{1}{m_i m_{i'}}\Delta\phi_{\substack{i\,i'\\ \alpha\alpha'}}^{nn'}, \quad (9)$$

the Green's matrix of the crystal with a defect is obtained from the Dyson equation

$$G = \left(1-G_0C\right)^{-1}G_0. \quad (10)$$

There are two possibilities to determine the vibration energies of a crystal containing a defect. The first is to calculate the difference of the densities of phonon states (DDPS) between the perturbed crystal $g(\omega)$ and the perfect crystal $g_0(\omega)$, which is given in matrix notation by

$$\Delta g(\omega) = g(\omega) - g_0(\omega) = \frac{1}{\pi}\mathrm{Im}\left\{\mathrm{Tr}\left\{\frac{\mathrm{d}G_0}{\mathrm{d}\omega^2}C\left(1-G_0C\right)^{-1}\right\}\right\}, \quad (11)$$

where ImTr denotes the imaginary part of the trace of the matrix. This equation can be used to determine localized modes and resonances inside the host-mode bands and LVMs outside the host-mode bands. The second possibility is to calculate defect induced singularities of the Green's function *i.e.* the zeros of the secular equation

$$\det\left\{1-G_0C\right\} = 0, \quad (12)$$

which can only be used to calculate LVMs outside the host-mode bands. It can be shown [9] that only small matrices are involved in equations (11, 12), the dimension of which are determined by the non-zero part of the perturbation matrix equation (9).

We calculated the Green's matrix equation (6) using the $\mathbf{k}$-vector summation over the Brillouin zone with the analytical tetrahedron method of Lehmann and Taut [10] and the special method described by Kaprzyk and Mijnarends [11], because this method avoids the singularity problem.

## 3 Calculation of the dynamical matrix

The interatomic force constants $\phi_{\substack{i\,i'\\ \alpha\alpha'}}^{nn'}$ and $\Phi_{\substack{i\,i'\\ \alpha\alpha'}}^{nn'}$ between component $\alpha$ of atom $ni$ and component $\alpha'$ of atom $n'i'$ of the perfect crystal and of the perturbed crystal respectively, are calculated using density-functional theory in the local density approximation. Because frozen phonon calculations can only be performed on special points in the Brillouin zone, we use the following scheme: One atom of a supercell is moved away from its equilibrium position. The resulting Hellman-Feynman forces on the other atoms are linear to the displacement, if the disposition is small enough. However, because of the plain-wave method used, the supercell is repeated an infinite number of times in all three space directions. If one atom is moved in one cell, it is also moved in all the copies of that cell. The result is a superlattice of displaced atoms. To separate force constants for individual atom pairs, the long range interaction, which is a dipole-dipole interaction, is subtracted from the results of the *ab initio* run. The results are force constants, which describe the sum of all force constants between a given atom and those atoms of the the superlattice of displaced atoms, that lie within a cut-off radius. By choosing different supercell geometries, individual force constants can be determined by reducing the set of all calculated force constant combinations, see reference [3] for the details.

The dynamical matrices of GaAs and cubic GaN were calculated including all forces up to the eleventh nearest neighbours, totalling in 72 different individual parameters due to symmetry requirements. The long-range electrostatic interaction was determined by an Ewald summation and the effective charge was fitted to reproduce the experimental splitting of the optical phonons at the $\Gamma$-point [2]. In case of the perturbed crystal the force constants depend considerably on the relaxation of the atoms around the defect [12].

We used a modified computer program originating from the Fritz-Haber-Institut Berlin [13] optimized for the massive parallel Cray computer. We use plane wave expansions and fully separable pseudo potentials of the Troullier-Martins scheme [14] in case of 3*d*-valence electrons and of the Bachelet-Hamann-Schlüter-Chiang scheme in case of 3*d*-core electrons. In the latter case a non-linear core correction for the exchange and correlation potential was included. We found practically no differences in the results for GaN between the calculations with 3*d*-core electrons and 3*d*-valence electrons. The supercell contained between 40 and 96 atoms and one special $\mathbf{k}$ point in the Brillouin zone was used, but no significant changes were found with four special points. For GaAs, full convergence was reached with a cut-off energy about 60 Ry, but most of the calculations were performed at about 33 Ry, leading to slightly stronger forces. We used 80 Ry for GaN with 3*d*-valence electrons and 40 Ry for GaN with 3*d*-core.

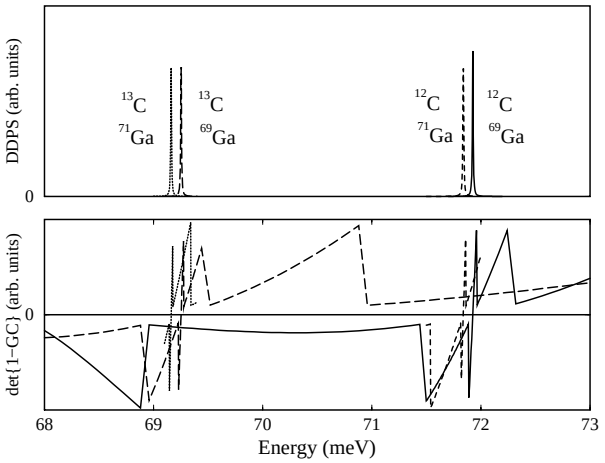


**Fig. 1.** Calculated LVMs of GaAs:C from the difference of the density of phonon states (upper part) and from the real part of the secular equation (12) (lower part). The solid line is for $^{12}C^{69}Ga_4$, the dotted line for $^{12}C^{71}Ga_4$, the long dashed line for $^{13}C^{69}Ga_4$, and the short dashed line for $^{13}C^{71}Ga_4$.

## 4 Local vibrational mode at GaAs:C

The system GaAs:$C_{As}$ shows a remarkable isotopic fine structure of a LVM well above the optical phonon band and has been extensively studied experimentally and theoretically [12,15–17]. The calculation of the Green's function of the perfect GaAs crystal was done using 240 **k** vectors in the irreducible part of the Brillouin zone and followed the line described in reference [2]. The atomic masses of the perfect crystal were taken from the natural isotope distribution to be $m_{Ga} = 69.7$ a.u. and $m_{As} = 74.9$ a.u. To set up the perturbation matrix we used the force constants from *ab initio* calculations reported in reference [12], taking interactions up to the second nearest neighbours into account. The results of our calculation of the LVM for the impurity isotopes $^{12}$C and $^{13}$C and for all of the four nearest neighbour isotopes $^{69}$Ga or $^{71}$Ga using equations (11, 12) are shown in Figure 1. Both methods gave the same energies for the LVMs and isotope shifts, which are summarized and compared with experimental values in Table 1. The difference between the calculated and observed energies of the LVMs is below 1% and is probably due to the approximations adopted here, *e.g.* the limited number of calculated force constants and the harmonic approximation. Due to the smaller values of the isotope shifts $\Delta$C and $\Delta$Ga, their relative difference to the observed values is accordingly larger.

The energies of the LVMs may also be compared with the results of the cluster calculations reported in reference [12]. Because we used in both cases the same force constants from the *ab initio* calculations, the differences originate from the finite size of the cluster of 489 vibrating atoms around the defect. The energy of the LVM was about 4% smaller than from the Green's function method, but the impurity isotope shift $\Delta$C came out about the same and the ligand induced isotope shift $\Delta$Ga was closer to the experimental value.

**Table 1.** Comparison of the calculated energies of LVMs with the observed values of reference [16] together with the isotope shifts. Here $\Delta$C denotes the isotope shift between $^{13}$C and $^{12}$C having four nearest neighbours $^{69}$Ga and $\Delta$Ga the ligand induced isotope shift of four $^{71}$Ga and four $^{69}$Ga as neighbours, which is the same for both of the carbon isotopes. All energies are in meV.

| | $^{12}$C, $^{69}$Ga | $^{13}$C, $^{69}$Ga | $\Delta$C | $\Delta$Ga |
|---|---|---|---|---|
| this work | 71.9 | 69.3 | 2.6 | 0.04 |
| exp. [16] | 72.3 | 69.7 | 2.60 | 0.03 |

Our method to calculate the energy of a LVM and its isotope shifts can therefore be used to identify the defect. Such LVMs can be considered as the result of a perturbation of the perfect lattice by the point defect, and the energy of the LVM is determined by the change of mass and by the change of the interatomic forces in the vicinity of the defect site. Although the change of mass is taken into account exactly, a correct energy does not necessarily mean that all the force constants had been calculated correctly. However, the isotope shift of the energy of the LVM $\hbar\omega$ with respect to an impurity or ligand atom mass $M$ is directly connected with the relative vibration amplitude $A/\sqrt{M}$ of that particular atom by the general formula

$$\frac{M}{\hbar\omega}\frac{\mathrm{d}\hbar\omega}{\mathrm{d}M} = -\frac{1}{2}A^2 \quad \text{with} \quad 0 \le A^2 \le 1. \tag{13}$$

Here $A^2$ is the sum of the squares of the three corresponding components of the normalized eigenvector of the dynamical matrix, which belongs to the LVM. Because the vibration amplitude of a particular atom depends on the interatomic forces between this atom and its neighbours, correct isotope shifts can only be calculated from correct interatomic forces entering the dynamical matrix.

## 5 Arsenic impurity in gallium nitride

The interest focussed on defects in GaN is due to their importance for the performance of optoelectronic devices in the blue spectral region. Siegle *et al.* [18,19] measured the Raman scattering at cubic GaN layers grown on GaAs or sapphire substrates. They observed eight low energy lines inside the acoustical phonon band of GaN between 11.8 meV and 31.0 meV. These lines were exclusively seen on GaAs substrates and they ruled out the possibility of attributing them to shallow donors so that they might be associated with LVMs at deep defects in the GaN layer or in the GaAs substrate. No further Raman lines other than GaN or GaAs phonons were observed. Their detailed analysis of the lines at 7.2 meV, 11.8 meV, 12.7 meV, 15.5 meV, 18.7 meV, 23.3 meV, 27.4 meV, 29.1 meV, and 31.0 meV gave no hints about the chemical nature of the defects, except that they must be specific for the growing process of GaN layers on GaAs substrates.

Because of the possibility of interdiffusion of arsenic into the GaN layer we investigated the As impurity in cubic GaN and examined, whether the much larger mass

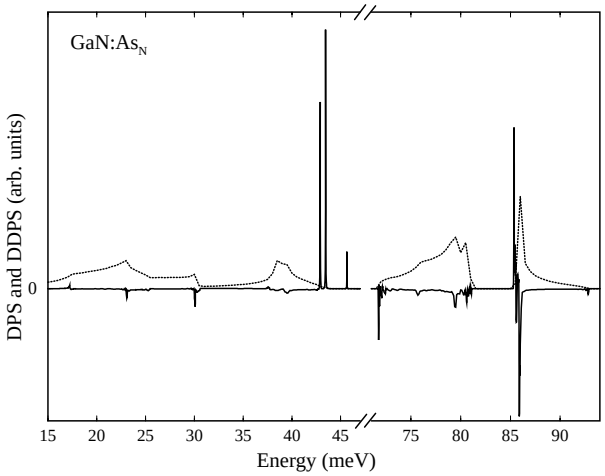


**Fig. 2.** Difference of the density of phonon states (DDPS) between the perturbed and the perfect GaN crystal, solid line. The dotted line shows the density of phonon states (DPS) of the perfect cubic GaN crystal.

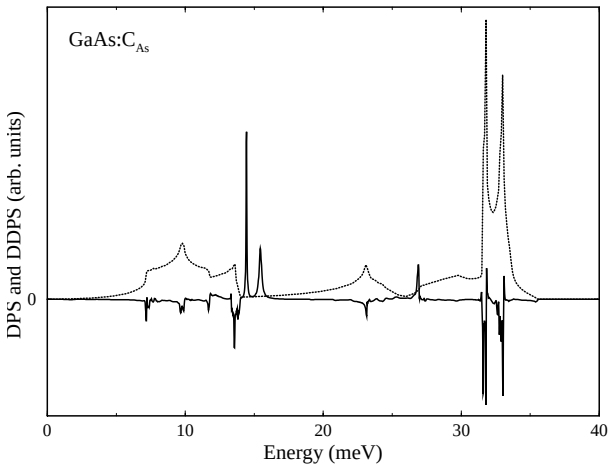


**Fig. 3.** Difference of the density of phonon states (DDPS) between the perturbed and the unperturbed GaAs crystal, solid line. The dotted line shows the density of phonon states (DPS) of the perfect cubic GaAs crystal.

of As compared with the replaced N atom generates low energy localized modes at this defect. We therefore calculated the modes induced by an isolated As impurity at a nitrogen site in cubic GaN crystals and applied the *ab initio* calculation of the phonon dispersion curves of reference [2]. Troullier-Martins pseudo potentials [14] were used and the Ga-3*d* electrons were treated as valence electrons so that convergence was achieved with a cut-off energy of 80 Ry. We calculated the Green's function from the eigenvalues and eigenfunctions of the dynamical matrix of the perfect GaN crystal using 505 **k** vectors in the irreducible part of the Brillouin zone by the tetrahedron method.

We took the relaxation at the As impurity up to the second nearest neighbours into account and calculated all force constants between the As atom and its relaxed first and second nearest neighbours by using a supercell of 54 atoms, which is $3 \times 3 \times 3$ times the size of the primitive cell. These force constants together with the force constants of the perfect GaN crystal were used to set up the perturbation matrix.

The resulting density of phonon states (DPS) of the perfect GaN crystal and of the difference of the density of phonon states (DDPS) due to the As impurity are shown in Figure 2. There are several peaks inside and outside the phonon bands of the host crystal and a number of resonances. The striking result is the appearance of a LVM in the band gap at 45.6 meV and two localized modes at 42.9 meV and 43.4 meV inside but near the upper edge of the acoustical phonon band. Because none of these modes had been seen in the Raman spectrum [19], we rule out the possibility of a perceptible amount of As impurities in the cubic GaN crystals in the layer. It is therefore very unlikely that the observed low energy Raman modes are associated with this defect. This has also been concluded from our cluster calculations of reference [6]. In the low energy region of the observed Raman peaks between 7.2 meV and 31.0 meV our calculated DDPS of Figure 2 also shows four resonances at 17.2 meV, 23.1 meV, 25.3 meV, and 30.1 meV. Their energies, however, are associated with specific energies of the DPS of the perfect GaN crystal, they show no isotope shift and have also been found from different impurities. In contrast to the resonances the localized modes at 42.9 meV and 43.4 meV are shifted by 0.2 meV/nucleon if the four nearest Ga neighbours are replaced by their isotopes. As a consequence, the resonances can not give an indication to As impurities, in spite of the fact that the resonance at 17.2 meV is close to the observed Raman peak at 18.7 meV.

## 6 Interpretation of the Raman lines of a GaN layer on a GaAs substrate

In order to understand the observed low energy Raman peaks between 7.2 meV and 31.0 meV [19], we calculated the localized modes and resonances of the carbon impurity on arsenic site in GaAs. The resulting DDPS is shown in Figure 3. The localized vibrations at 14.4 meV and 15.4 meV are caused by the carbon impurity, which was probably absent in the samples used. We found an isotope shift of 0.2 meV/nucleon for both of the lines if the four nearest Ga neighbours were replaced by their isotopes and 0.02 meV/nucleon for the impurity isotope shift. But the resonances between 7.2 meV and 33.0 meV, which do not show any isotope shift, are characteristic for the DPS of the perfect crystal and are approximately at the same energies for different defects, which might be present in the samples. We compiled our results of the resonances and localized modes in GaAs and cubic GaN in Table 2 and compared them with the measured Raman peaks at the GaN layer on a GaAs substrate. The higher energy resonances of Figure 2 at 71.7 meV, 78.5 meV, 80.6 meV, 85.4 meV, 85.9 meV, and 92.8 meV, which had also been

**Table 2.** Resonances and localized modes inside the phonon bands of GaAs and inside the acoustical phonon bands of cubic GaN in comparison with the observed Raman peaks at a GaN layer on a GaAs substrate. All energies are in meV.

| GaAs:C | | GaN:As | | GaN/GaAs |
|---|---|---|---|---|
| resonance | loc. mode | resonance | loc. mode | exp. [19] |
| 7.2 | | | | 7.2 |
| 9.6 | | | | |
| 11.7 | | | | 11.8 |
| 13.6 | | | | 12.7 |
| | 14.4 | | | |
| | 15.4 | | | 15.5 |
| | | 17.2 | | 18.7 |
| 23.1 | | 23.1 | | 23.3 |
| | | 25.3 | | |
| 26.9 | | | | 27.4 |
| | | 30.1 | | 29.1 |
| 31.7 | | | | 31.0 |
| 33.0 | | | | |
| | | 37.5 | | |
| | | 39.5 | | |
| | | | 42.9 | |
| | | | 43.4 | |

obtained from cluster calculations at slightly different energies [6], are not included in Table 2.

We conclude from Table 2 that the observed low energy Raman peaks of reference [19] are most probably due to resonances in the phonon bands of the GaAs substrate, which might be caused by defects near the interface between the GaN layer and the GaAs substrate. The calculated resonance at 33.0 meV could also not be seen in the Raman spectrum because of the TO phonon of the perfect GaAs crystal at approximately the same energy. It may also be the case that the observed lines at 18.7 meV and 29.1 meV are due to resonances of cubic GaN caused by different defects. More detailed investigations are necessary to confirm this assignment.

## 7 Conclusion

We presented an *ab initio* calculation of interatomic forces, which can be used to determine the vibrational Green's functions of the perfect and perturbed crystal from first principles. This allows not only the calculation of LVMs in the energy gap or above the optical phonon band, but also to determine pronounced peaks of the difference of the densities of phonon states between the perturbed and the unperturbed crystal, which can be associated with deep defects. In addition, the calculated impurities induce specific resonances inside the phonon bands, the energetic position of which is characteristic for the host crystal and practically does not depend on the chemical nature of the defect. The crucial points are the correct calculation of the phonons of the perfect crystal, of the relaxation of the atoms around the defect, and of the interatomic forces in the vicinity of the defect. The accuracy of the results of the Green's function technique can be improved by reducing the approximations adopted here and by increasing the computational effort. A direct deduction from the peaks of the DDPS to observed Raman peaks is, however, difficult.

The feasibility of the method has been demonstrated by the calculation of split-off modes of carbon impurities in GaAs, which are in good agreement with observation. The low energy Raman peaks, observed at a layer of cubic GaN on a GaAs substrate, can be interpreted as defect induced resonances of the GaAs substrate and of cubic GaN crystals.

The authors are grateful to Matthias Scheffler for the provision of the computer program. We thank the Konrad-Zuse-Zentrum für Informationstechnik Berlin and the Zentraleinrichtung Rechenzentrum of the Technische Universität Berlin for their support and the provision of computing facilities.

## References

1. P. Giannozzi, S. de Gironcoli, P. Pavone, S. Baroni, Phys. Rev. B **43**, 7231 (1993).
2. K. Petzke, C. Schrepel, U. Scherz, Z. Phys. Chem. **201**, 317 (1997).
3. K. Petzke, Phys. Rev. B (accepted).
4. D.A. Robbie, M.J.L. Sangster, P. Pavone, Phys. Rev. B **51**, 10489 (1995).
5. D.A. Robbie, M.J.L. Sangster, E.G. Grosche, R.C. Newman, T. Pletl, P. Pavone, D. Strauch, Phys. Rev. B **53**, 9863 (1996).
6. K. Petzke, C. Göbel, C. Schrepel, P. Thurian, U. Scherz, Mater. Sci. Forum **258-263**, 1179 (1997).
7. W. Frank, C. Elsässer, M. Fähnle, Phys. Rev. Lett. **74**, 1791 (1995).
8. A. Maradudin, Rep. Prog. Phys. **28**, 331 (1965).
9. J. Bernholc, S.T. Pantelides, Phys. Rev. B **18**, 1780 (1978).
10. G. Lehmann, M. Taut, Phys. Stat. Sol. (b) **54**, 469 (1972).
11. S. Kaprzyk, P.E. Mijnarends, J. Phys. C **19**, 1283 (1986).
12. K. Petzke, C. Göbel, C. Schrepel, U. Scherz, Mater. Sci. Forum **258-263**, 861 (1997).
13. R. Stumpf, M. Scheffler, Comp. Phys. Commun. **79**, 447 (1994).
14. N. Troullier and J.L. Martins, Phys. Rev. B **43**, 1993 (1991).
15. W.M. Theis, K.K. Bajaj, C.W. Litton, G.W. Spitzer, Appl. Phys. Lett. **41**, 70 (1982).
16. R.S. Leigh, R.C. Newman, M.J.L. Sangster, B.R. Davidson, M.J. Ashwin, D.A. Robbie, Semicond. Sci. Technol. **9**, 1054 (1994).
17. R.C. Newman, E.G. Grosche, M.J. Ashwin, B.R. Davidson, D.A. Robbie, R.S. Leigh, M.J.L. Sangster, Mater. Sci. Forum **258-263**, 1 (1997).
18. H. Siegle, I. Loa, P. Thurian, G. Kaczmarczyk, L. Filippidis, A. Hoffmann, C. Thomsen, D. Schikora, M. Hankeln, K. Lischka, Z. Phys. Chem. **200**, 187 (1997).
19. H. Siegle, A. Kaschner, P. Thurian, A. Hoffmann, I. Broser, C. Thomsen, Mater. Sci. Forum **258-263**, 1197 (1997).
20. C. Göbel, C. Schrepel, U. Scherz, P. Thurian, G. Kaczmarczyk, A. Hoffmann, Mater. Sci. Forum **258-263**, 1173 (1997).